ARCHIVES OF ELECTRICAL ENGINEERING VOL. 68(2), pp. 245–263 (2019)

DOI 10.24425/aee.2019.128266

HVDC auxiliary emergency power control strategy for power disturbance in two different positions of AC/DC interconnection system

CONGSHAN LI[1], PING HE[1], YOUYI WANG[2], YUYI JI[1], CUNXIANG YANG[1]

[1] *Zhengzhou University of Light Industry, China*

[2] *Nanyang Technological University, Singapore*
e-mail: 2015018@zzuli.edu.cn

(Received: 02.08.2018, revised: 14.01.2019)

Abstract: High voltage direct current (HVDC) emergency control can significantly improve the transient stability of an AC/DC interconnected power grid, and is an important measure to reduce the amount of generator and load shedding when the system fails. For the AC/DC interconnected power grid, according to the location of failure, disturbances can be classified into two categories: 1) interconnected system tie-line faults, which will cause the power unbalance at both ends of the AC system, as a result of the generator rotor acceleration at the sending-end grid and the generator rotor deceleration at the receiving-end grid; 2) AC system internal faults, due to the isolation effect of the DC system, only the rotor of the generator in the disturbed area changes, which has little impact on the other end of the grid. In view of the above two different locations of disturbance, auxiliary power and frequency combination control as well as a switch strategy, are proposed in this paper. A four-machine two-area transmission system and a multi-machine AC/DC parallel transmission system were built on the PSCAD platform. The simulation results verify the effectiveness of the proposed control strategy.

Key words: unbalanced power, emergency control, power angle stability, frequency stability, control logic

1. Introduction

HVDC emergency control is an auxiliary control measure, which can significantly improve the transient stability of an AC/DC interconnected system [1]. Through the power regulation characteristics of a DC system, it can suppress power angle oscillation [2, 3] and maintain the stability of power system frequency [4]. In terms of designing an auxiliary damping controller, there are mainly two kinds of designing methods, one is a model-based method, and the other is

a model-free method [5]. For these model-based methods, because the system order is very high, the mathematical model of the system usually has to be obtained through the identification method [6]. Recently, extensive research has been carried out to propose power oscillation damping and maintain the frequency stability of the interconnection system applying the Lyapunov theory [7], sliding mode control [8], model predictive control [9, 10], neuro-fuzzy feedback linearization [11], and auto disturbance rejection control [12]. In terms of using the feedback signal, it mainly includes frequency signals and power signals, with the application of wide-area measurement systems (WAMS) in power systems [13], it becomes possible to use the inertial center signal for wide area damping control [14]. In recent years, wind power has been vigorously developing all over the world. A new subsynchronous oscillation phenomenon in a wind farm integrated with a modular multilevel converter based HVDC transmission system has been recently found in the real world [15]. Nevertheless, wind farms and HVDC coordinated control can be utilized to improve system damping [16]. For a multiple HVDC transmission system, multiple HVDC coordinated control can be used to damp the system oscillation [17]. Optimal coordination of a multiple HVDC link system using centralized and distributed control is examined in [18]. A constraint factor of emergency power support of HVDC systems is investigated in [19]. Although many experts and scholars have studied HVDC auxiliary control to damp system oscillations and improve grid frequency stability in many aspects, none of the above studies has distinguished the location of disturbances (i.e. no distinction has been made between tie-line faults and AC system internal faults). Because the fault location is different, the DC auxiliary control strategy is different.

The power imbalance of the AC/DC interconnected system can be divided into two categories based on the disturbance location: 1) tie-line faults of an interconnected system. It leads to a simultaneous power imbalance at the sending-end and the receiving-end, i.e., the sending-end has excess power, and the receiving-end has insufficient power. It is obvious that this kind of unbalanced power can cause the generator rotor acceleration at the sending-end grid and the generator rotor deceleration at the receiving-end grid; 2) AC system internal faults. Obviously, for this kind of power imbalance, due to the isolation effect of the DC system, only the rotor of the generator in the disturbed area changes, and there is almost no influence on the AC system at the other end.

For the above two locations of power disturbance, it is generally different when making the auxiliary emergency control strategy. Especially for the internal faults of the AC system, the frequency stability constraints of the normal operation of the grid at the other end should be taken into consideration when formulating the strategy. As far as the current research is concerned, there is almost no difference in the formulation of emergency power control strategies and control objectives. Therefore, this paper makes an in-depth analysis of these two different locations of power disturbance, and puts forward effective emergency control strategies suitable for the two situations. The validity of the proposed method is verified by the simulation of a four-machine two-area transmission system and a multi-machine AC/DC parallel transmission system.

2. Analysis of emergency power support mechanism

When studying the transient stability of a power system under fault conditions, the system is often equivalent to a two-machine instability mode. The system is divided into the critical group S and the remaining group A, so the problem of the power angle stability of the system becomes

the relative oscillation of the critical group S to the remaining group A. The transient equations of the critical group S and the remaining group A are as follows:

$$\begin{cases} \dot{\delta}_S = \omega_S \\ \dot{\omega}_S = \dfrac{1}{M_S}\displaystyle\sum_{i\in S}[P_{mi} - P_{ei}] \end{cases}, \tag{1}$$

$$\begin{cases} \dot{\delta}_A = \omega_A \\ \dot{\omega}_A = \dfrac{1}{M_A}\displaystyle\sum_{i\in A}[P_{mj} - P_{ej}] \end{cases}, \tag{2}$$

where

$$\begin{cases} \delta_S = \dfrac{1}{M_S}\displaystyle\sum_{i\in S} M_i\delta_i, & \delta_A = \dfrac{1}{M_A}\displaystyle\sum_{i\in A} M_j \\ \dot{\omega}_S = \dfrac{1}{M_S}\displaystyle\sum_{i\in S} M_i\omega_i, & \dot{\omega}_A = \dfrac{1}{M_A}\displaystyle\sum_{j\in A} M_j\omega_j \\ M_S = \displaystyle\sum_{i\in S} M_i, & M_A = \displaystyle\sum_{i\in A} M_j \end{cases}, \tag{3}$$

where: M_S and M_A are the equivalent inertial time constant of the critical group S and remaining group A, respectively; δ_S and δ_A are the power angle under the inertial center of S and A, respectively; ω_S and ω_A are the angular frequency under the inertial center of S and A, respectively; P_{mi} and P_{ei} are the mechanical power and the electromagnetic power of the i unit under the inertial center of S, respectively; P_{mj} and P_{ej} are the mechanical power and the electromagnetic power of the j unit under the inertial center of A, respectively.

Combined Eq. (1) and Eq. (2), the transient state equation of the two machine system can be equivalent to a single machine system, and the rotor motion equation of the equivalent single machine system is

$$\begin{cases} \dot{\delta}_{SA} = \omega_{SA} \\ \dot{\omega}_{SA} = \dfrac{1}{M_S}\displaystyle\sum_{i\in S}[P_{mi} - P_{ei}] - \dfrac{1}{M_A}\displaystyle\sum_{i\in A}[P_{mj} - P_{ej}] \end{cases}, \tag{4}$$

where: $\delta_{SA} = \delta_S - \delta_A$, $\omega_{SA} = \omega_S - \omega_A$. For the above equivalent single machine system, when the system steady operation, $\dot{\omega}_{SA}$ is 0. When a fault occurs, due to the generator rotor inertia, the system can't guarantee the mechanical power and the electromagnetic power is equally instantaneous, thus, leads to the acceleration or deceleration of the generator rotor, and then ω_{SA} is not 0. If there are no effective control measures taken on time, it will lead to the continuous increase of δ_{SA} and eventually exceed the stable operation point of the system, which will cause the system to lose stability.

If the amount of DC power modulation is considered as mechanical power, when the system is subjected to disturbances, through DC auxiliary emergency control, Eq. (4) becomes

$$\begin{cases} \dot{\delta}_{SA} = \omega_{SA} \\ \dot{\omega}_{SA} = \dfrac{1}{M_S}\displaystyle\sum_{i\in S}[(P_{mi} + \Delta P_m) - P_{ei}] - \dfrac{1}{M_A}\displaystyle\sum_{i\in A}[(P_{mj} - \Delta P_m) - P_{ej}] \end{cases}, \tag{5}$$

where ΔP_m is the DC emergency power modulation.

For tie-line faults, by adjusting the power of other normal running DCs, making ΔP_m equal to the power of the faulty tie-line, it can ensure that ω_{SA} equals 0. The mechanism of DC emergency power support can be explained by the expansion of an equal area rule, as showed in Fig. 1.

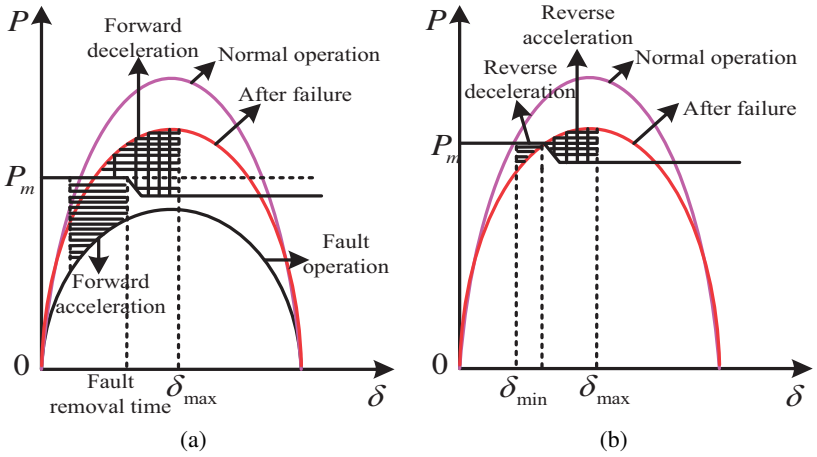

Fig. 1. Mechanism of DC emergency power support

The system is divided into four phases in each oscillation cycle after the fault: forward acceleration, forward deceleration, reverse acceleration and reverse deceleration.

In the first two stages, increasing the DC power can reduce the equivalent mechanical power P_m, thereby reducing the positive pendulum acceleration area and increasing the forward pendulum deceleration area; in the latter two stages, the returning DC power can make the equivalent mechanical power P_m increase, thereby reducing the swing back acceleration area and increasing the swing back deceleration area.

3. Analysis of power disturbance in two different positions

For an AC/DC interconnected power system, once the tie-line fails, it causes the power of both the sending-end and the receiving-end unbalanced. That is, during the transient process of the power grid, the mechanical power at the sending-end is greater than the electromagnetic power, and the electromagnetic power of the receiving-end is greater than the mechanical power. On the sending-end, the rotor of the generator will be accelerated and the frequency of the power grid will increase. On the receiving-end, the rotor of the generator will be decelerated and the frequency of the power grid will be reduced. If it is an internal failure of the AC system, because of the isolation of the DC system (i.e. the DC system is generally constant power control), the rotor speed of the generator is changed only in the disturbed area, and the other end of the power grid is almost unaffected.

For one of the tie-line faults, the basic strategy for DC emergency power control is to use the DC overload capability in parallel with it to urgently increase the DC power and transfer the power of the faulty DC to the normal operating DC system as much as possible, so as to achieve the purpose of maintaining the power balance of the sending-end grid and receiving-end grid.

The above-mentioned emergency power control strategy for tie-line faults does not necessarily apply to the internal failure of the AC system, and the appropriate power support strategy should be established according to the capacity of the grid at the other end. It is divided into two kinds of situations: 1) if the capacity of the normal operation grid at the other end is infinite, then the DC emergency control strategy can be the same as the above tie-line faults, that is to say, the unbalanced power under power grid fault conditions will be transferred to the normal power grid as soon as possible. Due to the very large capacity of the normal operating grid, the unbalanced power transferred from the outside has little effect on the grid. The frequency of the normal power grid can still keep close to the stable equilibrium point, and the normal power grid can be regarded as a buffer node. Obviously, the infinite capacity grid is just the ideal model, and the real power grid is a limited capacity grid; 2) For the other end grid is a limited capacity grid, due to the fact that the unbalanced power needs to be rapidly consumed on the faulty power grid. If using the same power control strategy that will cause a large amount of the unbalanced power transfer to the normal power grid, it will have a certain impact on the normal power grid. In this case, it is necessary to consider the stability constraints of the normal grid during the formulation of the emergency power control strategy, that is, the amount of the unbalanced power transfer must be constrained by the stability of the normal operating grid. The above analysis can be clearly expressed in Fig. 2.

Previous studies did not distinguish between these two kinds of unbalanced states. That is, the same power control strategy was adopted for the power disturbances of the two different locations. Usually, the frequency difference or power angle difference between the two ends of the power grid are the control target. The above control strategy is unreasonable for one end of the grid with limited capacity.

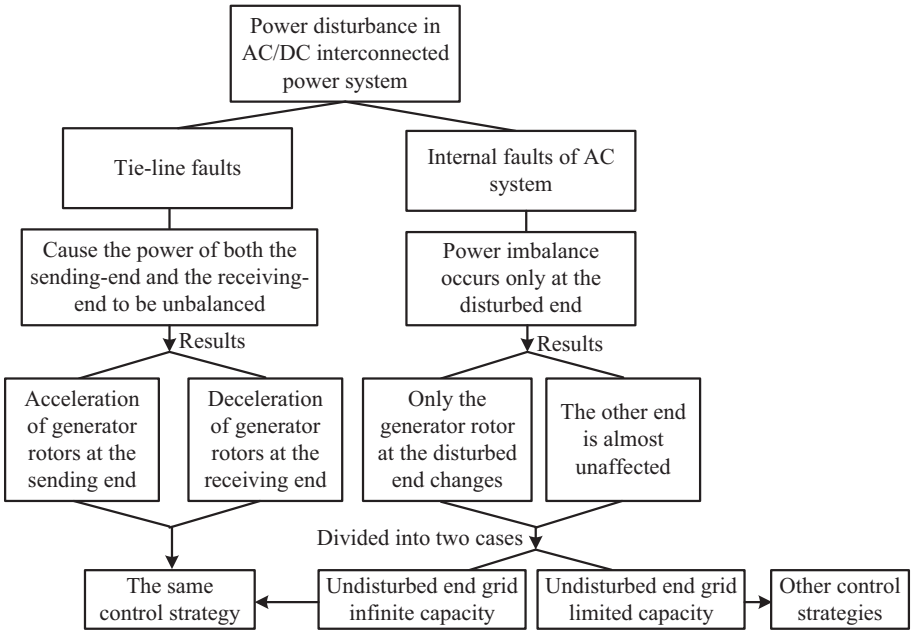

Fig. 2. Analysis of power disturbance in two different positions

4. Auxiliary control strategy design

4.1. Design of auxiliary controller

For an AC/DC transmission system, a DC auxiliary controller design must meet the following three requirements: 1) when the tie-line fails. The DC transmission system connected in parallel uses its overload capability to smoothly transfer the power of the fault line to this line. If the power of the fault line is lower than the overload power of the DC line, all the power of the fault line should be transferred to the DC system. On the contrary, if the transmission power of the fault line is higher than the overload power of the DC line, the DC system uses the extremum control, namely the maximum overload operation state; 2) when a disturbance occurs in the AC system, an HVDC should be able to adjust the power output according to the change of frequency, to maintain system stability; 3) after the fault is eliminated, the HVDC system should be run in accordance with the rated power level.

In order to fulfil the above requirements, and make full use of the DC power modulation function, select the appropriate AC and DC state variables, to achieve emergency power support and auxiliary frequency control functions. This paper designs a DC auxiliary power/frequency controller (APFC) considering the stability constraints of a normally operating end grid, which is based on the DC emergency power support (DCEPS) as the foundation, and joins in the auxiliary frequency control (AFC) modulation. The principle of the DC APFC structure is shown in Fig. 3, and the principle of the AFC control is shown in Fig. 4.

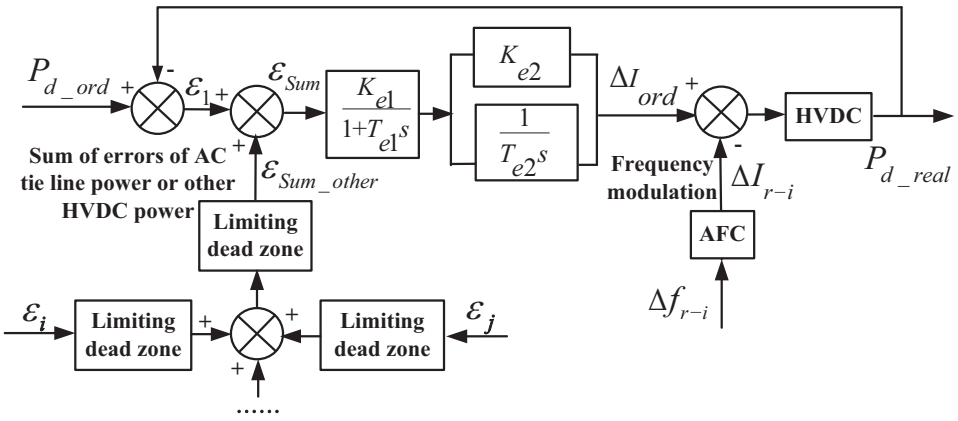

Fig. 3. Simplified block diagram of APFC

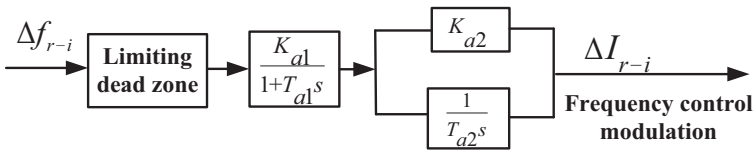

Fig. 4. AFC control schematic

Fig. 3 shows the simplified block diagram of the APC closed-loop control of the HVDC, and the transfer function of the APC can be expressed as:

$$\begin{cases} \Delta I_{ord} = \dfrac{K_{e1}}{1+T_{e1}s}\left(K_{e2}+\dfrac{1}{1+T_{e2}s}\right)\varepsilon_1, & \varepsilon_{Sum\_other} < e_1 \\ \Delta I_{ord} = \dfrac{K_{e1}}{1+T_{e1}s}\left(K_{e2}+\dfrac{1}{1+T_{e2}s}\right)\varepsilon_{Sum}, & \varepsilon_{Sum\_other} \geq e_1 \end{cases} . \tag{6}$$

Among them, ε_{Sum} represents the sum of the power errors of all the AC and DC tie lines, ε_{Sum_other} represents the sum of the power errors of other AC and DC tie lines except this DC power, K_{e1} and T_{e1} are the parameters of the first order lag, K_{e2} and T_{e2} are the PI controller parameters. In Fig. 3, the limiting dead zone is added before the power error of each tie line, be sure to act only when the tie line fails, to avoid the normal operation of the AC or DC power in the slight disturbance resulting in the DC power unnecessary fluctuation. The transfer functions of ΔI_{r-i} are

$$\begin{cases} \Delta f_{r-i} = f_r - f_i \\ \Delta I_{r-i} = \dfrac{K_{a1}}{1+T_{a1}s}\left(K_{a2}+\dfrac{1}{T_{a2}s}\right)\Delta f_{r-i}, & |\Delta f_{r-i}| \geq e_2 \\ \Delta I_{r-i} = 0, & |\Delta f_{r-i}| < e_2 \end{cases} , \tag{7}$$

where: f_r and f_i are the frequency of the sending end grid and receiving end grid, respectively; Δf_{r-i} is the frequency difference between the sending end grid and receiving end grid; K_{a1} and T_{a1} are the parameters of the first order lag link; K_{a2} and T_{a2} are the parameters of the PI controller. The function of the AFC setting limiting dead zone is the same as the APC.

4.2. Analysis of limiting factors for emergency power control

The DC system can achieve the power boost value according to the power lifting command, which is mainly dependent on the level of AC system bus voltage, which is essentially due to the HVDC need to consume a large amount of reactive power when lifting power that causes a bus voltage drop. Thus, the result in the DC system unable to complete the power increase according to the power setting value and the limiting factor is directly related to the strength of the AC system.

For the limitation of the bus voltage level in the AC system, the voltage sensitivity factor (VSF) is defined in this paper to evaluate the limitation of the AC system bus voltage level on power lifting capacity. Specifically defined as:

$$|\Delta f_{Normal}| < 0.5 \text{ Hz}, \tag{8}$$

where: ΔU is the AC bus voltage drop caused by the increase of DC power; U_N is the rated bus voltage value of the AC system; F_{VSF} can be obtained by a small disturbance in the system. Therefore, when the lifting power is ΔP, the bus voltage drop in the AC system is

$$\Delta U_{Total} = \frac{\Delta P \cdot F_{VSF}}{U_N} . \tag{9}$$

Therefore, the constraint condition of the actual system power lifting capacity ΔP_{dc_A1} can be expressed as:

$$\begin{cases} \Delta P_{dc\_A1} = \dfrac{\Delta U_{Total} \cdot F_{VSF}}{U_N}, & |\Delta U_{Total}| < \Delta U_{\max} \\ \Delta P_{dc\_A1} = \dfrac{\Delta U_{\max} \cdot F_{VSF}}{U_N}, & |\Delta U_{Total}| \geq \Delta U_{\max} \end{cases}, \tag{10}$$

where $\Delta U_{\max}$ is the maximum allowable range of voltage fluctuation.

Another limitation factor to increase the power is the transmission capacity of the DC system itself. In general, DC has 1.5 times short-term overload capacity and 1.1 times long-term overload capacity. In addition to the overload operation, the DC transmission system has the minimum power limit, this is decided by the minimum current limiting factor of the DC system. The limitation of the DC system's transmission capacity can be achieved by limiting amplitude. Constraints can be expressed as:

$$\begin{cases} P_{\min} \leq P_{Actual} = 1.1 \cdot P_N, & \Delta t \geq 3 \text{ s} \\ \Delta P_{dc\_A2} = 0.1 \cdot P_N, & \Delta t \geq 3 \text{ s} \\ P_{\min} \leq P_{Actual} = 1.5 \cdot P_N, & \Delta t < 3 \text{ s} \\ \Delta P_{dc\_A2} = 0.5 \cdot P_N, & \Delta t < 3 \text{ s} \end{cases}, \tag{11}$$

where: $P_{\min}$ is the minimum DC power, P_{Actual} is the actual transmission power of the DC system. P_N is the rated power of the DC system, ΔP_{dc_A2} is the amount of modulation limited by the system itself, Δt is the power boost time.

For the AC system faults, the stability constraints of the normal operation grid at the other end is taken into account when performing auxiliary power/frequency design. Because the actual power grid is the bounded capacity grid. The frequency stability constraint condition of the normal operation grid of the other end is

$$|\Delta f_{Normal}| < 0.5 \text{ Hz}, \tag{12}$$

where Δf_{Normal} represents the system frequency variation of the normal grid caused by the DC power modulation. Therefore, under the frequency stability constraint of the normal grid, the DC power modulation ΔP_{dc_A3} is

$$|\Delta P_{dc\_A3}| < \frac{|\Delta f_{\max}|}{f_N} \cdot P_{N\_C}, \tag{13}$$

where P_{N_C} is the capacity of the normal operation grid at the other end. $\Delta f_{\max}$ is the maximum frequency fluctuation value of the power grid, which generally is 0.5 Hz. f_N is the rated frequency of the power grid. It is necessary to explain that the above constraints do not take into account the effects of a generator governor and load characteristics on frequency regulation. The influence of the generator governor and load characteristics on the frequency regulation can be expressed by defining a frequency sensitive factor (FSF), which is defined as

$$F_{FSF} = \frac{\Delta P}{P_{N\_C}}, \tag{14}$$

where F_{FSF} is a frequency sensitive factor. Therefore, taking into account the generator governor and load characteristics and taking into account the frequency stability constraints of the normal operation grid, the DC power modulation amount is

$$\begin{cases} \Delta P_{dc\_A3} = P_{N\_C} \cdot F_{FSF}, & |F_{FSF}| < \Delta f_{\max} \\ \Delta P_{dc\_A3} = P_{N\_C} \cdot F_{\max}, & |F_{FSF}| \geq \Delta f_{\max} \end{cases}. \tag{15}$$

Therefore, considering the constraints of multiple factors we can say that the final DC power modulation can be expressed as:

$$\Delta P_{\max} = \min\left(\Delta P_{dc\_A1}, \Delta P_{dc\_A2}, \Delta P_{dc\_A3}\right). \tag{16}$$

4.3. Auxiliary power/frequency strategy considering multiple factor constraints

In order to further explain the working principle of the APFC in detail, the four-machine two-area two-DC parallel transmission system is taken as an example for illustration, the system structure diagram is shown in Fig. 5.

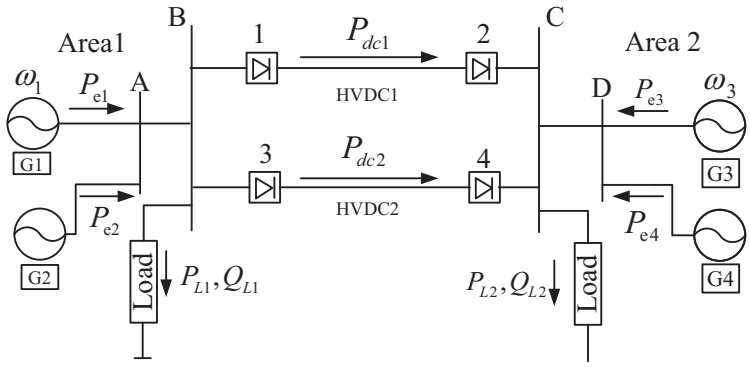

Fig. 5. Four-machine two-area parallel transmission system

There are two generators on the sending-end and the receiving-end, respectively, and there are two parallel DC transmission systems. The P_{dc1} transmission power is 113.5 MW, the P_{dc2} transmission power is 53.5 MW, P_{L1} is 529 MW, Q_{L1} is 61 MVAR, P_{L2} is 385 MW, Q_{L2} is 55 MVAR. The HVDC system is modified by a CIGRE model, and its parameters are identical to the CIGRE model except that the conversion ratio of a converter transformer is different. Detailed system parameters are shown in Table 1.

When one of the DC systems fails, the other DC system's APC and AFC control modules are simultaneously put into operation and the power of the fault DC is transferred to the normal DC system so as to achieve the purpose of stabilizing the whole interconnected system. When the sending-end or receiving-end is disturbed, the APC control module is shielded, and only the AFC module is used to power modulation to realize the frequency stability of the sending-end and the receiving-end. The auxiliary control logic block diagram is presented in Fig. 6.

Table 1. Main parameters of the employed system

Generator	G1 = G2	G3 = G4	Ratio	HVDC1
Rated kV	11.547	11.547	Rectifier side	230/46
Rated kA	26.8	27.02	Inverter side	230/45
H(s)	6.5	6.175	Ratio	HVDC2
$\mathbf{X_d(pu)}$	1.8	1.6	Rectifier side	230/23
$\mathbf{X'_d(pu)}$	0.3	0.2	Inverter side	230/23
Xq(pu)	1.7	1.5	–	–
$\mathbf{X'_q(pu)}$	0.228	0.2	–	–
$\mathbf{T'_{d0}(s)}$	8	6	–	–
$\mathbf{T'_{q0}(s)}$	0.85	0.65	–	–

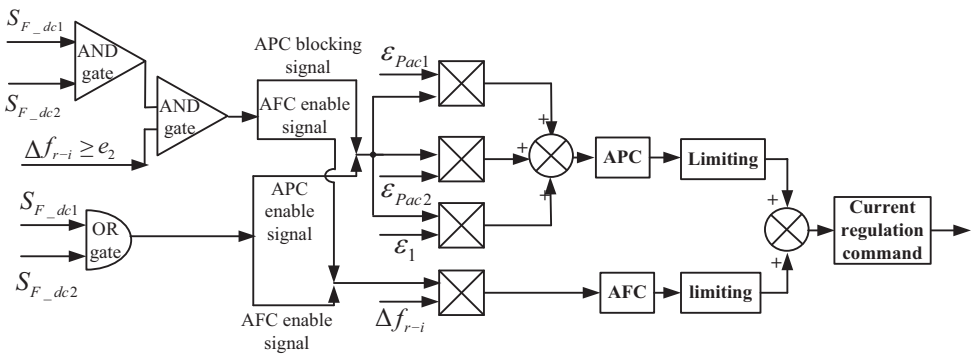

Fig. 6. APFC control logic diagram

In Fig. 6, $S_{F\_dc_1}$ and $S_{F\_dc_2}$ are faulty signals of DC tie-line, respectively, there are two states, 1 and 0, respectively. 1 represents fault signal and 0 represents non fault signal. The detail logic is as follows:

1. When both $S_{F\_dc_1}$ and $S_{F\_dc_2}$ are 0, and $|\Delta f_{r-i}| \geq e_2$ is 1, it means that the tie-line has not failed and the AC system has been disturbed. The APC control module is shielded and only the AFC control module is put into operation.

2. When $S_{F\_dc_1}$ or $S_{F\_dc_2}$ is 1, the APC and AFC control modules are launched at the same time.

4.4. APFC controller parameter setting

This paper adopts the Ziegler-Nichols integral method and an empirical method to implement an APFC parameters setting. The parameter setting should be considered according to the role it plays in the APFC, an APC's main function is to realize the control of a fault DC power transfer.

It is necessary to consider the impact of large-scale power flow transfer on the sending end and the receiving end grid, therefore we cannot move towards the goal too fast. The role of the AFC is to realize the transfer of unbalanced power from one end of the power grid to the other end of the power grid, so the control speed can be faster than that of the APC.

The Ziegler-Nichols tuning method is the theoretical calculation method, which needs to know the mathematical model of the system, so this paper adopts a small disturbance test method to obtain the system input and output curves. The Total Least Squares-Estimation on Signal Parameters via Rotational Technique (TLS-ESPRIT) method is used to determine the mathematical model of the system. The specific steps are as follows:

1) creating a mathematical model identification system,

2) determining the theoretical value of the parameters by the Ziegler-Nichols method,

3) considering the specific role of an APFC according to the engineering experience, repeated debugging and determining the final parameters.

The mathematical model of the two order system is obtained by the identification method.

$$G(s) = \frac{-0.0047s^2 - 0.0064s}{s^2 + 0.0651s + 9.4973}. \tag{17}$$

The final controller parameters are shown in Table 2.

Table 2. Parameters of APFC controller

APC Parameters	K_{e1}	T_{e1}	K_{e2}	T_{e2}
	1	0.05	1	2
AFC Parameters	K_{a1}	T_{a1}	K_{a2}	T_{a2}
	1	0.025	0.5	10

5. Simulation analysis

In order to verify the effectiveness of the proposed method, a four-machine two-area power grid and multi-machine AC/DC parallel power grid are simulated respectively, the system structure of the four-machine two-area power grid is showed in Fig. 5.

5.1. Simulation of four-machine two-area power grid

Firstly, a four-machine two-area classical power grid example is simulated, and three kinds of faults are set up for simulation analysis.

1. Case 1: set to HVDC2 to permanent lock failure at 3 seconds. The power curves of HVDC1, the angular frequency difference curves of the generator rotors 1 and 3, and the frequency change curves of the AC system on both sides are separately simulated, the simulation results are compared with the amplitude adaptive emergency power support control method [20], as shown in Figs. 7 and 8. In the legend, No means no auxiliary control, APC means only auxiliary power

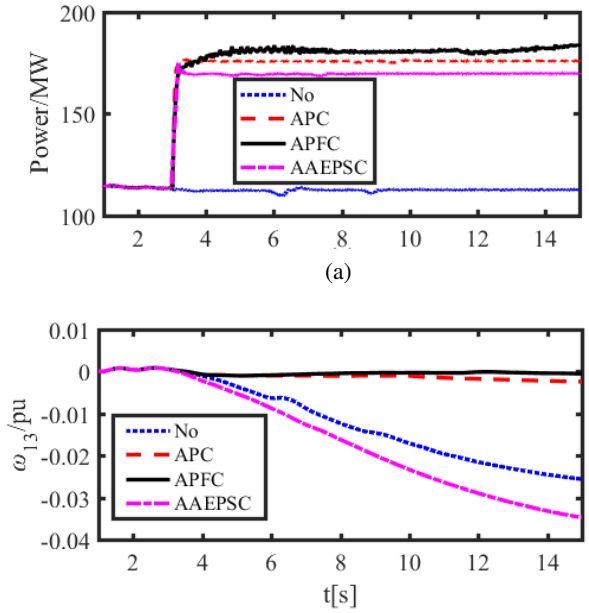

Fig. 7. (a) HVDC1 power curves; (b) angular frequency difference curves

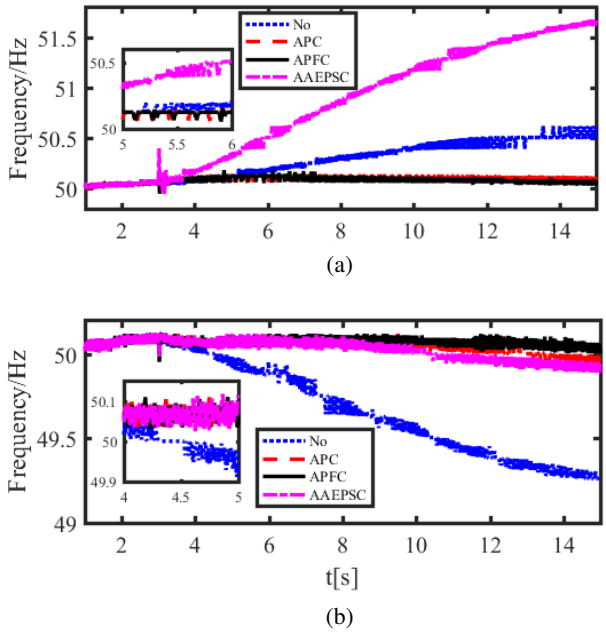

Fig. 8. (a) Rectification side bus frequency; (b) inverter side bus frequency

control, APFC means combined auxiliary power and auxiliary frequency control, AAEPSC means amplitude adaptive emergency power support control, the same means as the following:

It has to be explained that for the tie-line faults, according to the power support strategy of this paper, the APC and AFC control modules act simultaneously to complete the emergency control. In order to be compared with previous studies, we simulated the control effect when only the APC control module was put into operation.

As shown in Figs. 7 and 8, both of the APFC control and AFC control can quickly improve the DC power, restrain the change of the power angle of the generator, and stabilize the frequency of the AC system. The AAEPSC can maintain the frequency stability of the receiving power grid well, but it has little effect on maintaining power angle stability. Compared with the control of the APFC and APC, it is found that the APC control module plays a significant role in the connection line fault, and the AFC control is equivalent to the fine tuning function on the basis of the APC control. Due to the addition of the AFC control, the control effect of the APFC is slightly better than the APC control and AAEPSC.

2. Case 2: a feeder branch of the sending-end grid was set to fail at 3 seconds. The circuit breaker is tripped, and the faulty branch was removed, leading to the loss of 10 MW loads. Similarly, power curves of HVDC1, the angular frequency difference curves of generator rotors 1 and 3, and the frequency change curves of the AC system on both sides are separately simulated. They are shown in Figs. 9 and 10.

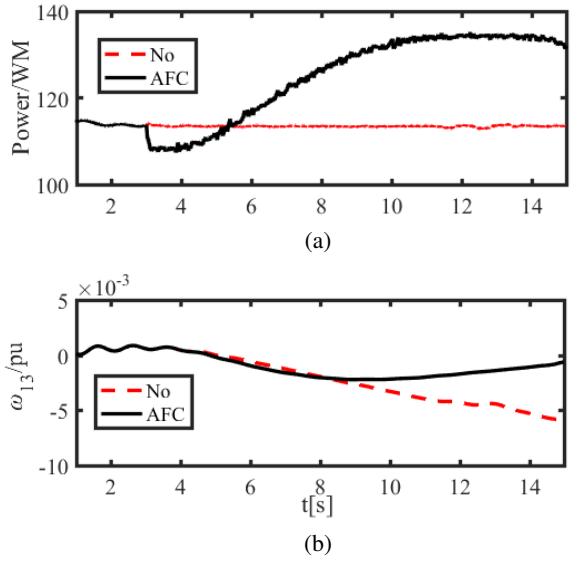

Fig. 9. (a) HVDC1 power curves; (b) angular frequency difference curves

As it can be seen from Fig. 9 through the action of the AFC, the angular velocity deviation of the generator is effectively suppressed. It can be seen from Fig. 10 that the frequency of the sending-end power grid is lower than that of the unassisted control when there is auxiliary control, and the frequency of the receiving-end power grid is higher when there is the auxiliary control, than when there is no auxiliary control, but through the AFC function, in the end, the frequency of both sides of the grid is maintained within the normal range.

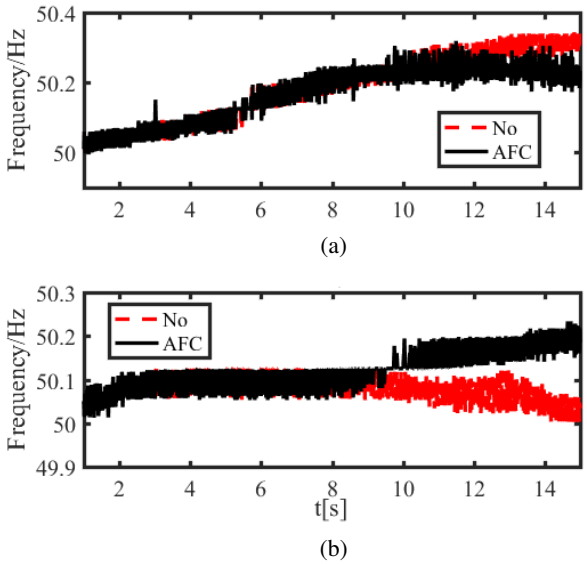

Fig. 10. (a) Rectification side bus frequency; (b) inverter side bus frequency

3. Case 3: set the same fault as case 2, but the failure results in the loss of 50 WM load. Similarly, the power curves of HVDC1, the angular frequency difference curves of generator rotors 1 and 3, and the frequency change curves of the AC system on both sides are separately simulated. They are shown in Figs. 11 and 12.

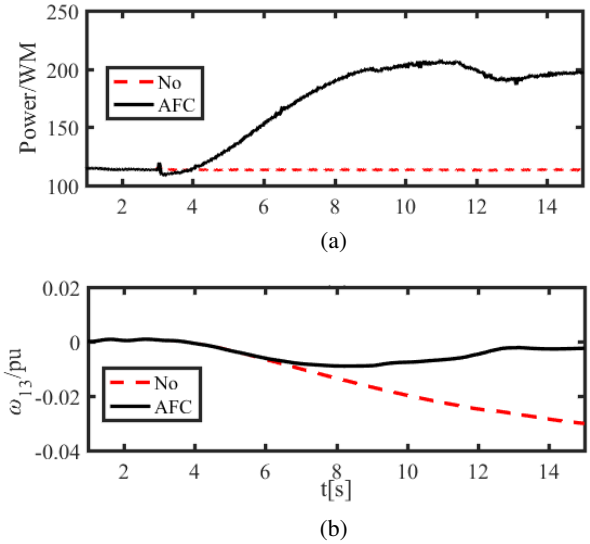

Fig. 11. (a) HVDC1 power curves; (b) angular frequency difference curves of the generator rotors 1 and 3

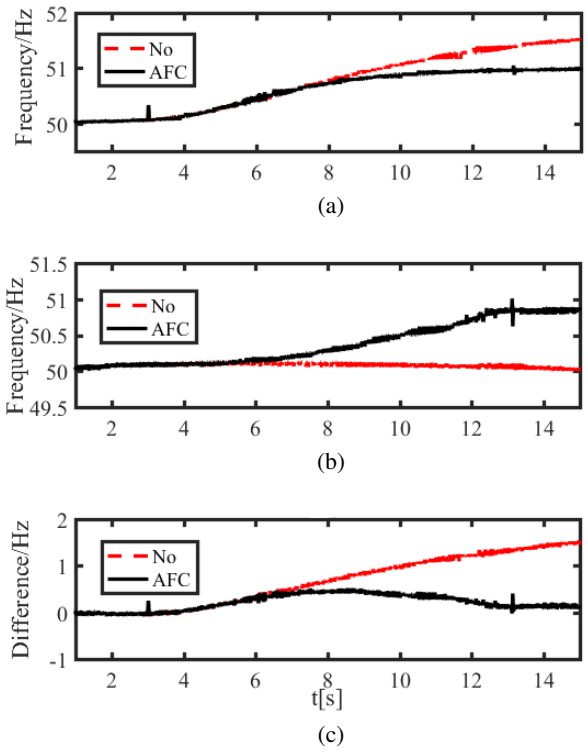

Fig. 12. (a) Rectification side bus frequency; (b) inverter side bus frequency; (c) bilateral frequency difference curves

From Fig. 11, it can be observed that the generator's angular velocity deviation ω is effectively suppressed by the AFC control. From Fig. 12, it can be observed that the frequency difference between the two sides of the AC power grid is almost 0 when there is the AFC control. However, by comparing the frequency curves of the sending-end and receiving-end, it can be seen that due to the large excess power of the sending-end power grid, although the auxiliary angle control can suppress the power angle oscillation and realize the goal that the frequency difference between the two sides of the power grid is 0, but due to the AFC control, resulting in both sides of the grid, frequency has exceeded the stability constraints of the normal grid. Obviously, for the internal fault of the AC system, the frequency stability constraint of the normal grid at the other end must be taken into account when formulating the AFC control strategy. Therefore, considering the constraint of frequency stability at the other end, transfer power of DC will be reduced, and only one end of the grid will achieve frequency stability. For this kind of large power disturbance caused by the internal fault of the AC system, only relying on the DC power transfer control can not realize the frequency stability of both ends of the grid at the same time, so it must be coordinated with other control measures, such as machine control. Due to space limitations, this article no longer elaborates on coordination control.

5.2. Simulation of multi-machine AC/DC parallel power grid

In order to further verify the applicability of the proposed method, the multi-machine AC/DC parallel transmission system (that is, a practical power grid) is simulated. The system structure diagram is shown in Fig. 13. Thermal power plants 1, 2 and 3 have two generators, one generator and three generators respectively, and hydroelectric power plants 1 and 2 have four generators respectively.

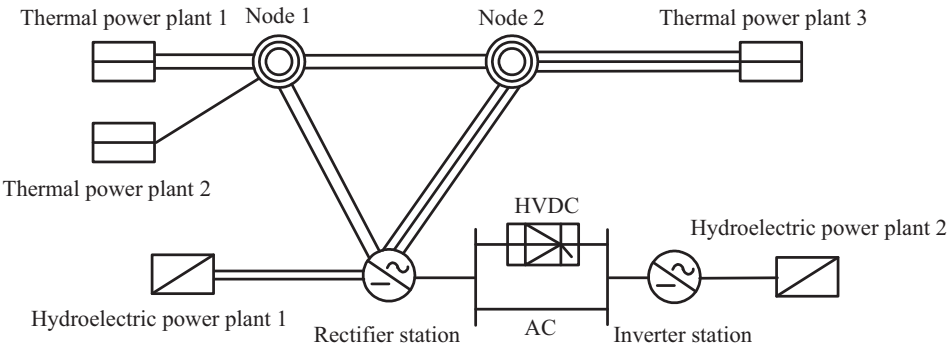

Fig. 13. Multi-machine AC/DC parallel transmission system

Setting the AC tie-line in parallel with the HVDC causes transient fault in 3 seconds, and farther 3.5 seconds resume normal power supply. The power angle difference of the hydropower units on both sides of the HVDC and the rectification side as well as the inverter side bus frequency are the observation targets, the simulation results are compared with the AAEPSC, as shown in Figs. 14, 15 and 16.

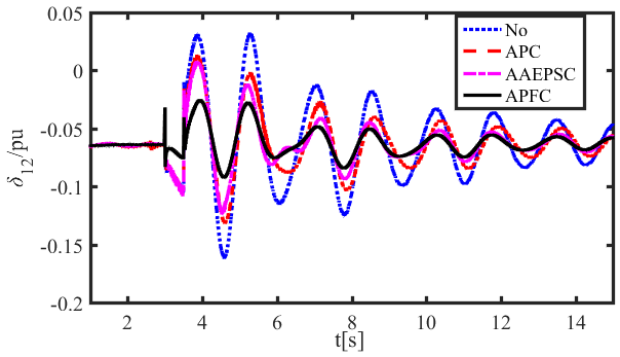

Fig. 14. Power angle difference curve

From the simulation of multi-machine AC/DC parallel transmission power grid, it can be seen that when the tie-line fault occurs, APFC control effect is also better than APC and APFC.

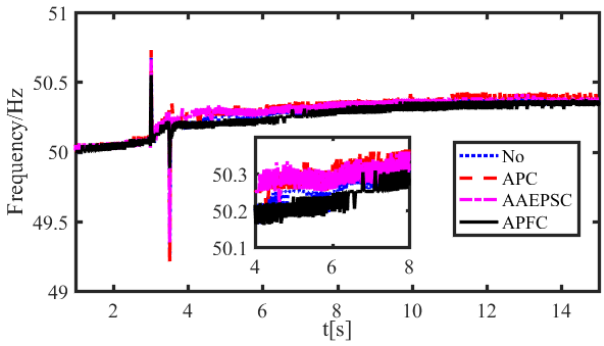

Fig. 15. Rectification side bus frequency

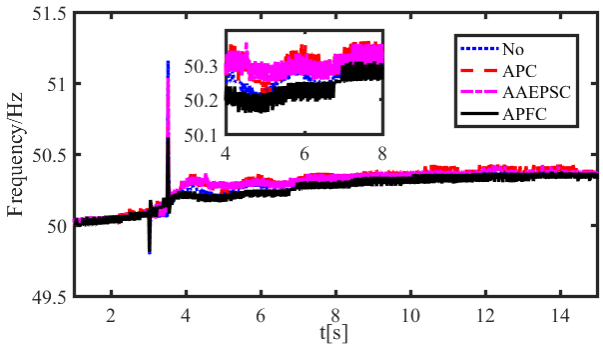

Fig. 16. Inverter side bus frequency

6. Conclusions

This paper proposes an emergency power control strategy for an AC/DC power system under power disturbance in two different locations to improve the stability of the AC/DC interconnected power system. The APFC combination control structure and logic switching control strategy are designed through the four-machine two-area transmission system and multi-machine AC/DC parallel transmission system simulation to verify the effectiveness of the method. The main conclusions are as follows:

1. For the tie-line faults, the joint control effect of the APC and AFC is better than that of the APC alone. Due to the addition of the AFC on the APC that can reflect changes in grid frequency, this is the main reason for which the APFC is superior to the APC.

2. For the power imbalance caused by internal disturbance of one end of the power grid, the frequency difference between the two sides of the power grid cannot be used as the only control target. When considering the power transfer control, the frequency stability constraint of the normal operation power grid at the other end must be considered. For small power disturbances, the frequency of both sides of the grid can be maintained within a stable range by using the AFC modulation of the DC. For larger power disturbances, the frequency stability of the two sides can't

be achieved at the same time only by the modulation of the AFC, and the maximum disturbance power transfer control can only be realized on the premise of ensuring the stability of the other end of the power grid, and other auxiliary control measures are needed to achieve the stability of the power grid.

The research results in this paper have some reference value for emergency control of a real power grid.

References

[1] Harnefors L., Johansson N., Zhang L. *et al.*, *Interarea oscillation damping using active-power modulation of multiterminal HVDC transmissions*, IEEE Transactions on Power Systems, vol. 29, no. 5, pp. 2529–2538 (2014).

[2] Rahman H.l., Khan B.H., *Stability improvement of power system by simultaneous AC-DC power transmission*, Electric Power System Research, vol. 78, iss. 4, pp. 756–764 (2008).

[3] Cai H., Qu Z., Gan D., *A nonlinear robust HVDC control for a parallel AC/DC power system*, Computers and Electrical Engineering, vol. 29, iss. 1, pp. 135–150 (2003).

[4] Jallad J., Mekhilef S., Mokhlis H., *Frequency Regulation Strategies in Grid Integrated Offshore Wind Turbines via VSC-HVDC Technology: A Review*, Energies, vol. 10, iss. 9, pp. 1244–1272 (2017).

[5] Shen Y., Yao W., Wen J. *et al.*, *Adaptive supplementary damping control of VSC-HVDC for interarea oscillation using GrHDP*, IEEE Transactions on Power Systems, vol. 33, no. 2, pp. 1777–1789 (2018).

[6] Eriksson R., Söder L., Zhang L., *Optimal coordinated control of multiple HVDC links for power oscillation damping based on model identification*, European Transactions on Electrical Power, vol. 22, no. 2, pp. 188–205 (2012).

[7] Eriksson R., *Coordinated control of multi terminal DC grid power injections for improved rotor angle stability based on Lyapunov theory*, IEEE Transactions on Power Delivery, vol. 29, pp. 1789–1797 (2014).

[8] Weng H., Xu Z., *WAMS based robust HVDC control considering model imprecision for AC/DC power systems using sliding mode control*, Electric Power System Research, vol. 95, pp. 38–46 (2013).

[9] Azad S.P., Iravani R., Tate J.E., *Damping Inter-Area Oscillations Based on a Model Predictive Control (MPC) HVDC Supplementary Controller*, IEEE Transactions on Power Systems, vol. 28, iss. 3, pp. 3174–3183 (2013).

[10] Fuchs A., Imhof M., Demiray T., Morari M., *Stabilization of Large Power Systems Using VSC–HVDC and Model Predictive Control*, IEEE Transactions on Power Delivery, vol. 29, iss. 1, pp. 480–488 (2014).

[11] Ahmad S., Khan L., *Performance Analysis of Conjugate Gradient Algorithms Applied to the Neuro-Fuzzy Feedback Linearization-Based Adaptive Control Paradigm for Multiple HVDC Links in AC/DC Power System*, Energies, vol. 10, no. 6, pp. 819–841 (2017).

[12] Li C.S., Liu T.Q., Liu L.B., *A auto disturbance rejection controller of multi-HVDC*, Transactions of China Electrotechnical Society, vol. 30, no. 7, pp. 10–17 (2015).

[13] Preece R., Milanovic J.V., Almutairi A.M., Marjanovic O., *Damping of inter-area oscillations in mixed AC/DC networks using WAMS based supplementary controller*, IEEE Transactions on Power Systems, vol. 28, iss. 2, pp. 1160–1169 (2013).

[14] Du Z., Zhang Y., Chen Z., *Integrated emergency frequency control method for interconnected AC/DC power systems using centre of inertia signals*, IET Generation, Transmission & Distribution, vol. 6, iss. 6, pp. 584–592 (2012).

[15] Lyu J., Cai X., Amin M. *et al*., *Subsynchronous Oscillation Mechanism and Its Suppression in MMC-Based HVDC Connected Wind Farms*, IET Generation, Transmission & Distribution, vol. 12, vol. 4, pp. 1021–1029 (2018).

[16] Pipelzadeh Y., Chaudhuri N.R., Chaudhuri B. *et al*., *Coordinated Control of Offshore Wind Farm and Onshore HVDC Converter for Effective Power Oscillation Damping*, IEEE Trans. Power Syst., vol. 32, no. 3, pp. 1860–1872 (2017).

[17] Mc Namara P., Negenborn R.R., De Schutter B., Lightbody G., *Optimal coordination of a multiple HVDC link system using centralized and distributed control*, IEEE Tran. Control Syst. Technol., vol. 21, iss. 2, pp. 302–314 (2013).

[18] Shen L., Barnes M., Preece R. *et al*., *The effect of VSC-HVDC control on AC system electromechanical oscillations and DC system dynamics*, IEEE Transactions on Power Delivery, vol. 31, no. 3, pp. 1085–1095 (2016).

[19] Weng H., Xu Z., Xu F., *Research on constraint factor of emergency power support of HVDC systems*, Proceedings of the CSEE, vol. 34, vol. 10, pp. 1519–1527 (2014).

[20] Liu C.R., Wei F.S., Chen Z.W. *et al*., *Magnitude Adaptive Emergency Power Support Control Technology*, Automation of Electric Power Systems, vol. 37, no. 21, pp. 123–128 (2013).